Environmental Science & Technology

Article

pubs.acs.org/est

Methane, Black Carbon, and Ethane Emissions from Natural Gas Flares in the Bakken Shale, North Dakota

Alexander Gvakharia,*[,†] Eric A. Kort,[†] Adam Brandt,[‡] Jeff Peischl,[§,∥] Thomas B. Ryerson,[∥] Joshua P. Schwarz,[∥] Mackenzie L. Smith,[†] and Colm Sweeney[§]

[†]Climate and Space Sciences and Engineering, University of Michigan, Ann Arbor, Michigan 48109, United States

[‡]Department of Energy Resources Engineering, Stanford University, Stanford, California 94305, United States

[§]Cooperative Institute for Research in Environmental Science, University of Colorado, Boulder, Colorado 80309, United States

[∥]NOAA ESRL Chemical Sciences Division, Boulder, Colorado 80305, United States

ABSTRACT: Incomplete combustion during flaring can lead to production of black carbon (BC) and loss of methane and other pollutants to the atmosphere, impacting climate and air quality. However, few studies have measured flare efficiency in a real-world setting. We use airborne data of plume samples from 37 unique flares in the Bakken region of North Dakota in May 2014 to calculate emission factors for BC, methane, ethane, and combustion efficiency for methane and ethane. We find no clear relationship between emission factors and aircraft-level wind speed or between methane and BC emission factors. Observed median combustion efficiencies for methane and ethane are close to expected values for typical flares according to the US EPA (98%). However, we find that the efficiency distribution is skewed, exhibiting log-normal behavior. This suggests incomplete combustion from flares contributes almost 1/5 of the total field emissions of methane and ethane measured in the Bakken shale, more than double the expected value if 98% efficiency was representative. BC emission factors also have a skewed distribution, but we find lower emission values than previous studies. The direct observation for the first time of a heavy-tail emissions distribution from flares suggests the need to consider skewed distributions when assessing flare impacts globally.

INTRODUCTION

Over 140 billion cubic meters (BCM) of gas is globally flared each year.[1] Flaring is used to dispose of gas at production and processing facilities that lack infrastructure and means to capture or use the gas. The United States flares about 8 BCM per year, with almost half of that coming from North Dakota alone.[2] From 2004 to 2014, the amount of gas annually flared in North Dakota increased from 0.08 to 3.7 BCM, and in 2014, about 28% of North Dakota's total produced natural gas was flared.[3] Flaring has implications for the atmosphere. Although ideally, gas would be captured instead of lost, it is preferable to flare rather than vent because flaring destroys methane (CH_4) and volatile organic compounds that affect air quality, converting them to CO_2. CH_4 is a potent greenhouse gas, the second-most-important anthropogenic greenhouse gas behind CO_2 based off integrated radiative forcing.[4,5] Flaring is not 100% efficient, and through incomplete combustion, it can be a source for CH_4 and VOCs.[6,7] Flaring can also create black carbon (BC) as a by-product, an anthropogenic forcer of climate with public health implications.[8−11] The World Bank recently introduced a "Zero Routine Flaring" initiative to end flaring worldwide by 2030 through government incentives and institutional cooperation, hoping to mitigate economic losses due to flaring and relieve its burden on the atmosphere.[12]

Inventories that account for flaring often use a combustion efficiency value of 98% of the initial gas, citing an EPA technical report.[13,14] This efficiency value assumes flare stability and can decrease based on wind speed and other factors such as flow rate or aeration. Studies have investigated flare efficiency in laboratories using scaled-down flare simulations in a controlled environment, reporting 98−99% flare combustion efficiency,[15,16] but there have been few field studies done to assess flare efficiency and directly measure emissions in a real-world environment. Thus, scaled-up laboratory results may not be representative of real-world flaring. A study of two flare sites in Canada calculated an average observed combustion efficiency of 68 ± 7%, much lower than the assumed efficiency.[17] One remote sensing study in The Netherlands found high efficiencies of 99% but only analyzed three flares, with up to

Received: October 12, 2016
Revised: April 10, 2017
Accepted: April 12, 2017
Published: April 12, 2017

DOI: 10.1021/acs.est.6b05183
Environ. Sci. Technol. 2017, 51, 5317−5325

30% error in the measured gas concentrations, and noted the lack of in situ data.[18] There was also a comprehensive study to observe industrial flare emissions and efficiency but the tests were conducted at a flare test facility, not directly at well sites.[19] To our knowledge, the only extensive study of in situ flare efficiency for CH_4 sampled ten flares in the Bakken Shale in North Dakota and one in western Pennsylvania.[20] This study reported high flare efficiencies up to 99.9%, but based on their identification techniques, they acknowledged a possible bias toward larger, brighter-burning, and thus more-efficient, flares.

Black carbon emissions from gas flaring have been investigated, but there are not many studies that use direct observations of flaring. Schwarz et al. (2015)[10] quantified total field emissions of BC and derived an upper-bound on BC emission factor for flaring from the Bakken using the same aircraft campaign data as used in this paper. Their emission factor was obtained using BC flux calculated with a mass balance technique for the entire field. Hence, it did not target individual flares. It includes all BC sources in the region (e.g., diesel trucks, generators, limited agriculture, etc.) and is expected to provide an upper bound. Weyant et al. (2016)[21] calculated BC emission factors from targeted flares in the same region and found an average value well below the upper bound of Schwarz et al. (2015), and, to our knowledge, this is the only previously published peer-reviewed study of BC emissions from flaring that directly sampled flares. BC emission factors have been shown to vary based on fuel chemistry and stability of the flare, necessitating the use of specific emission factors or a distribution rather than using a single average value as representative.[22]

The lack of direct, in situ observations of flaring efficiency suggests that estimates of emissions from incomplete combustion may be inaccurate. Also, using a single value for flaring emission factors or combustion efficiency does not take into account the various parameters that may affect a flare,[23] and a statistically robust sample of flaring efficiency would help identify a representative distribution. Total fugitive emissions from oil and gas production and leakage can be a substantial source of atmospheric CH_4 and are underrepresented in inventories.[24] Studies have observed non-normal distribution of CH_4 emissions in some fields, where less than 10% of sampled sources contributed up to 50% of the sampled emissions.[25−29] A study of flare emissions using Greenhouse Gas Reporting Program and Gas Emission Inventory data found that 100 flares out of 20 000 could be responsible for over half the emissions in the United States, but this conclusion results from the non-normal distribution of gas volume flared and not from a skewed flare combustion efficiency (which is not represented).[30] In addition to the non-normal distribution of gas volume flared, there may be a skewed distribution of emissions from incomplete combustion in flares based on efficiency as well.

We present an analysis of combustion efficiency and emission factors of CH_4, BC, and C_2H_6 for 37 distinct flares in the Bakken Shale Formation in North Dakota using data obtained during a May 2014 aircraft campaign, this being (to our knowledge) the largest study of flaring emissions in the field based on number of flares and the first to include C_2H_6. This gives us sufficient statistics to obtain an efficiency distribution and determine the implications for total fugitive emissions from incomplete combustion in actual field conditions.

METHODS

Flights and Instrumentation. All observations used in this analysis were made as part of the Twin Otter Projects Defining Oil−Gas Well Emissions (TOPDOWN 2014) study and were collected onboard a National Oceanic and Atmospheric Administration (NOAA) DHC-6 Twin Otter aircraft.[10,31,32] This campaign focused on understanding the atmospheric impact of fossil fuel extraction activities. A total of 17 research flights were conducted on 11 separate days between May 12−26, 2014, totaling 40 h. Flights were typically 3−3.5 h in duration and were primarily conducted at low-altitudes (400−600 magl) within the planetary boundary layer at an average speed of 65 m/s. Vertical profiles were performed in each flight to define the mixed layer height. Flights dedicated to mass balance conducted transects around the Bakken region, and although a few flares were sampled during these transects, most of the flares were identified on "mowing-the-lawn" flights that swept across the region to target point sources as well as some flights dedicated to point source identification. Flares were circled multiple times during these flights between 400 and 600 magl, although some were sampled higher up, around 1000 magl. Flares were not specifically targeted for any particular characteristic such as size, brightness, or flaring volume. Flares were sampled over the entire region rather than in a particular cluster, giving low spatial sampling bias. However, due to the nature of the sampling, brighter flares were more easily identifiable from the plane and, thus, more likely to have been targeted. Not all passes by a flare produced a well-defined peak that could be used in the efficiency analysis. Many of the flares were sampled at a distance on the order of hundreds of meters to kilometers downwind. This gave the flare plume time to disperse and allowed us to measure large plumes over a time period of 10−20 s, providing more data per plume than if we sampled closer and lower.

CH_4, CO_2, carbon monoxide (CO), and water vapor (H_2O) were measured with a Picarro 2401-m cavity ringdown spectrometer with a sampling rate of 0.5 Hz. CH_4 was measured with an accuracy of ±1.4 ppb and a precision of ±0.2 ppb, and CO_2 was measured with an accuracy of ±0.15 ppm and a precision of ±0.03 ppm.[33,34] An Aerodyne mini direct absorption spectrometer was used to continuously measure C_2H_6, deployed as described previously in literature[35,36] along with hourly measurements of a standard gas to confirm stability.[32] Sampling was conducted at 1 Hz with precision of <0.1 ppb and an average accuracy of ±0.5 ppb.[32] Due to the Aerodyne ethane instrument having a response time of 1 s, compared to the Picarro's 2 s response time, there were sharper, narrower peaks in C_2H_6 than CO_2 and CH_4. To enable a point-by-point comparison of C_2H_6 to CO_2, a weighted moving average (WMA) was applied to the C_2H_6 data. The total integrated value of the C_2H_6 peak did not significantly change with the WMA filter, indicating conservation of mass with the method.

All trace gases are reported as dry air mole fractions, converted from the measured wet air mole fractions using water vapor observations from the Picarro. A single-particle soot photometer (SP2 by Droplet Measurement Technology Inc., Boulder, CO) was used to measure refractory black carbon (rBC) for particles containing rBC in the mass range of 0.7−160 fg. The SP2 provided 1-s rBC mass-mixing ratios with systematic uncertainty of 25%.[10,37] A pair of differential GPS antennae on the fuselage of the Twin Otter provided aircraft

DOI: 10.1021/acs.est.6b05183
Environ. Sci. Technol. 2017, 51, 5317−5325

heading, altitude, latitude, longitude, ground speed, and course over ground. Wind speed was calculated as described in Conley et al. (2014),[38] with estimated uncertainties of ±1 m/s in magnitude and ±6° in direction. A Rosemount deiced Total Temperature Sensor, model number 102CP2AF, measured ambient temperature. Calibration before and after the field project indicate measurement performance with precision of ±0.2 °C and accuracy of ±1.0 °C.

Flare Identification. We identified flares in the following ways. During the science flights, all significant events were logged, including when the plane flew by a flare. These flight notes thus provide times when a flare was visually confirmed, and these flare plumes were identified in the data for the corresponding flight and flagged. After locating all the flares confirmed by the flight notes, we searched through the remaining data to find plumes that could be possible flares but were not noted during the flight, such as smaller flares that might have been hard to see on the ground. To identify the other possible flare plumes, we looked for peaks in CO_2 where ΔCO_2, the peak enhancement, was greater at its maximum point than 4σ of the CO_2 background variability, indicating a statistically significant elevation of CO_2 as a result of combustion from a flare. We also looked for a peak less than 20 s in time. At a mean ground speed of 65 m/s, this corresponds to a source about 3 km away using Gaussian plume theory,[39] which is about the distance we tended to sample where the plume still presented a robust signal above background. Figure 1 shows the research aircraft flight paths, known flare locations,[3] and where we sampled plumes.

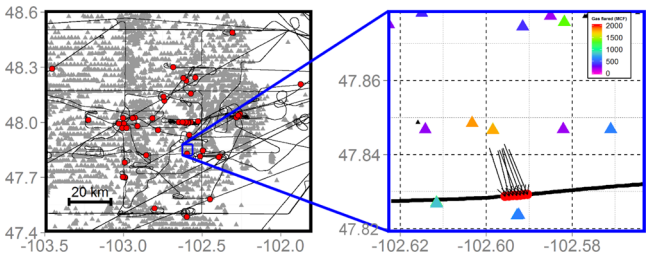

Figure 1. Left panel shows flight paths (black lines), wells with known flaring (gray triangles),[3] and flare plume locations (red points) from the TOPDOWN 2014 campaign in the Bakken field in northwest North Dakota. Times when the plane circled around an area multiple times to repeatedly sample can be seen in the middle of the region. Right panel is zoomed in on a single flare plume, with flight path (black line), flare plume (red points), and wells with reported flaring (filled triangles with corresponding monthly flaring amounts). The arrows indicate the wind direction. We used the wind direction, distance from well, and flaring amount to verify that the plume was caused by flaring.

To verify if these additional plumes identified in the data were indeed caused by flaring, we co-plotted the locations of these events with all nearby wells with reported flaring and other CO_2 producers such as processing facilities and gas plants using the EPA GHG Reporting Program as seen in Figure 1. Certain flare locations were cross-checked with additional data from the VIIRS Active Fire Map and North Dakota Oil and Gas ArcIMS Viewer. Then, using Gaussian plume theory, we estimated how far away the source of a plume was based on the plume width and wind conditions, matching the plume to a possible flare source.[39] Although the science flights were conducted on days with steady winds, leading to low variability in wind speed and direction, we accepted plumes that were within 20% of the theoretical distance to account for deviation in other factors such as not flying directly in the center of the diffused plume. If a plume was located downwind from a well with flaring, was not downwind of another CO_2 source, and had a width and distance consistent within 20% of Gaussian plume theory, we considered it likely due to a flare source. If a plume was not downwind of a flare at a distance consistent with Gaussian plume theory or had interference from another CO_2 source, we omitted it from the analysis. A total of 39 flare plumes were identified with the flight notes, and out of 17 additional plumes in the data, 13 were accepted using our verification method and 4 rejected for a total of 52 flare plumes from 37 unique flares.

Other sources for methane or black carbon closely colocated with flares (such as diesel engines or fugitive losses from production wells) could contribute to the observations we are attributing to flaring, and we assess their potential impact on our analysis here. Using gas composition data from over 550 samples, the average chemical plume from the Bakken was determined to be 0.7% CO_2, 3.7% N_2, 49% CH_4, 21% C_2H_6, and the rest in higher-order hydrocarbons.[40] This results in a molecular weight of about 29 g/mol, close to that of air and nearly double the weight of natural gas from other fields with higher CH_4 ratios.[21] An unburned source of gas is therefore neutrally buoyant compared to a hot flare exhaust plume, which will rise in the atmosphere.[41] However, the flare plume can entrain these other sources, mixing them as the buoyant plume rises in the atmosphere. If we assume a flare converts 98% of its hydrocarbons to CO_2, and that enhancements near a well pad due to other emissions are 50 ppm of CH_4 and 415 ppm of CO_2, then if the flare plume entrained a volume equal to its own (50% dilution), the resulting CH_4/CO_2 slope measured by the aircraft (see Figure 2) would change by less than 1%, smaller than the uncertainty range in fitting the slope. Considering typical values for methane and CO_2 enhancement (40 ppb and 5 ppm on average, respectively), we estimate the slope error (and, thus, the error on calculated emission factors) would be less than 1% with 10% as an upper bound. Adjusting the flare efficiency in this estimation does not significantly affect the result (using a 90% combustion efficiency, all else equal, would also have an impact of 1% on the slope). Although we cannot definitively rule out all potential contributions from such sources to the plumes we are analyzing, these considerations of possible entrainment suggest it is not significant in this analysis, though the potential impact would suggest our results may represent a lower bound for combustion efficiency.

Combustion Efficiency. Destruction efficiency and emissions factors were calculated for each flare sampled. Black carbon emission factors were determined following the methodology of Weyant et al. (2016)[21] using eq 1:

$$EF_{BC} = 1000 \times F\frac{C_{BC}}{C_{CO_2} + C_{CH_4} + C_{BC}} \quad (1)$$

Here, C_{CO_2}, C_{CH_4}, and C_{BC} are the mass concentrations of carbon in g/m^3 for each product with the respective background removed and F is the ratio of carbon mass to total hydrocarbon mass, calculated to be 0.79 from gas composition data for the Bakken.[40] CO_2 and CH_4 data were converted from molar ratios to g/m^3 using a molar volume at standard temperature and pressure (273 K, 1013 mb) to match

DOI: 10.1021/acs.est.6b05183
Environ. Sci. Technol. 2017, 51, 5317−5325

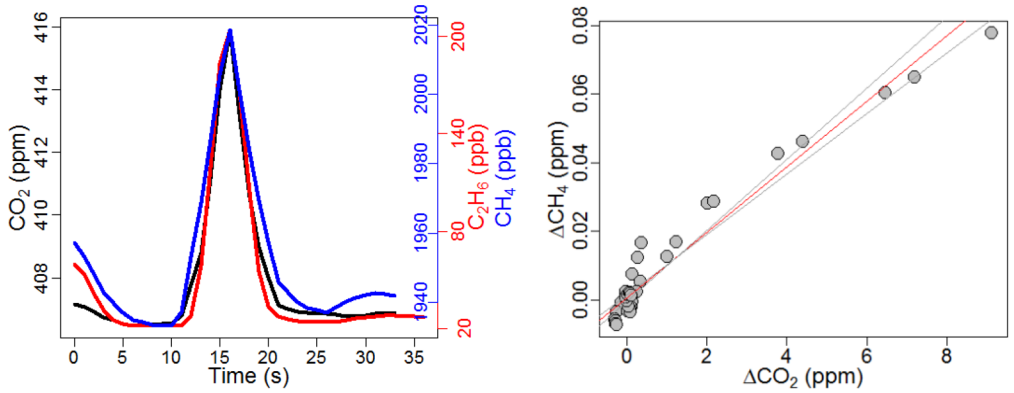

Figure 2. Example of a flaring plume with CO_2, CH_4, and C_2H_6 time series and regression to find CH_4 EF.

the conditions of the BC mass concentrations. This EF_{BC} value is given in grams of BC per kilogram of gas and can be converted to g/m^3 using a gas density of 1.23 ± 0.14 kg/m^3 for the composition.[40] For some of the flares we did not detect a strong BC enhancement correlated with CO_2, causing skewed or negative emission factor values. To account for this, when the peak enhancement ΔBC was below the detection limit of 4σ of the background, we used a value of half the detection limit in the EF calculation as in Weyant et al. (2016);[21] this was observed in a third of the plumes. The measured BC concentrations were scaled up by 15% to account for accumulation-mode mass outside of the SP2 detection range, as described in Schwarz et al. (2015);[10] rBC mass in either the coarse mode or a subaccumulation mode size range would not be accounted for by this adjustment. Generally, as in Schwarz et al. (2015),[10] the accumulation mode size distribution is well-fit with a log-normal function, and any additional smaller or larger populations of BC particles are revealed by deviations from the log-normal fit at the smaller or larger limits of the detection range, respectively. Here, there was no evidence of additional nonaccumulation modes.

Emission factors for CH_4 and C_2H_6 were obtained by first calculating the peak enhancement of CH_4, C_2H_6, and CO_2. We calculated a mean background value for each plume using the concentration data from 5 to 10 s before the start and after the end of the plume and then subtracted the background from the plume values to obtain ΔCH_4, ΔC_2H_6, and ΔCO_2. ΔCH_4 and ΔC_2H_6 were fit with a Reduced Major Axis (RMA) regression to ΔCO_2 for each peak to obtain the emission factor in ppm of CH_4 or C_2H_6 per ppm of CO_2.[20] Figure 2 shows an example plume from a flare and its CH_4 regression. Regressions were well-correlated with 10−20 data points in each flare plume. Uncertainty in EF for CH_4 and C_2H_6 was given by 95% confidence intervals from the regression. For all plumes, EF_{BC} from eq 1 linearly correlated with the slope of BC versus CO_2 with an R^2 of 0.97. This fit was used to derive uncertainty in EF_{BC} from 95% confidence intervals of the regression of BC and CO_2.

We calculated the destruction removal efficiency (DRE) following the methodology of Caulton et al. (2014)[20] using eq 2, with a small correction to report the value as the fraction of gas destroyed rather than remaining.

$$\mathrm{DRE}\,(\%) = \left(1 - \frac{\mu CH_4}{((X) \times \mu CO_2) + \mu CH_4}\right) \times 100 \qquad (2)$$

μCH_4 and μCO_2 are the gas concentrations in ppm, and X is the carbon fraction of CH_4 in the total fuel gas before combustion. From gas composition data for the field,[40] the value of X is 0.26 ± 0.05 for CH_4.

This DRE calculation was done two ways. First, by integrating over the entire peak to obtain a DRE value from the total integrated amount of CH_4 and CO_2. Second, by calculating the DRE value for each point in the peak individually to get an aggregate DRE data set as seen in Caulton et al. (2014).[20] The respective baseline values were removed from each gas concentration in both methods. Because the integral method calculates DRE using the average concentration over the sampling time of the gases in the plume, and the point-by-point mean represents the average instantaneous DRE, a significant divergence between the results would be indicative of a potential problem with the approach. For all flares, the integrated DRE differed from the mean point-by-point DRE by 1% on average, demonstrating robustness between the two methods. C_2H_6 DRE was also calculated using both methods, with $X = 0.23 \pm 0.03$ for C_2H_6. The effect of X's variability on the DRE is small and within the calculated uncertainty for DRE.

Detection Threshold. We compared the standard deviation of CH_4 background and the maximum peak CO_2 enhancement to calculate a "noise DRE" using eq 2 to assess the impact of a potential signal produced by background variability on the DRE. The distribution suggests a sensitivity threshold around 99%. We compared the sensitivity distribution to the measured DRE distribution, and an analysis of variance between the two produced a p value of 9×10^{-7}, suggesting that they are statistically significantly different. Thus, it would be difficult to distinguish measured DRE values of greater than 99% as significant compared to background variability, but values less than 99%, as we have observed, are robustly detectable with our approach. There is a trade-off between our sampling approach and the one used by Caulton et al. (2014),[20] where they flew lower and closer to the flares. With our flights, we obtained more points in each plume, allowing us to calculate regression lines for emission factors. However, we encountered a lower signal-to-noise ratio, making it more difficult to precisely measure the DRE of very efficient flares. We used the difference between 100% and the DRE calculated using the sensitivity as a proxy for DRE uncertainty in each individual flare.

DOI: 10.1021/acs.est.6b05183
Environ. Sci. Technol. 2017, 51, 5317−5325

RESULTS

Emission Factors. Figure 3 shows the calculated CH_4 and C_2H_6 emission factors plotted against mean aircraft-level wind speed for all flare plumes. Previous laboratory flare studies have observed a strong nonlinear dependence of inefficiency on crosswind speed,[15,16] and Caulton et al. (2014)[20] observed a weak relationship in the flares they sampled in the field. Considering our observed emission factors and crosswind speeds, we find similar results to Caulton et al. (2014). An exponential fit of our data suggests a weak dependence, with parts of the data possibly following different distinct curves. A Pearson correlation analysis of the data and the exponential fit produced a weak correlation coefficient (0.34). Gas exit velocity and flare parameters like the stack diameter can affect the inefficiency curve and may be the reason for the apparent presence of multiple curves, but unfortunately, these values were not known for our sampled flares. More-specific knowledge of the gas composition and flow rate would potentially be illuminating for the possible bimodal distribution in CH_4 EF of low-efficiency emitters (>30 ppb/ppm) and high-efficiency emitters (0−20 ppb/ppm), but we can only hypothesize without detailed information on specific flares at time of our sampling.

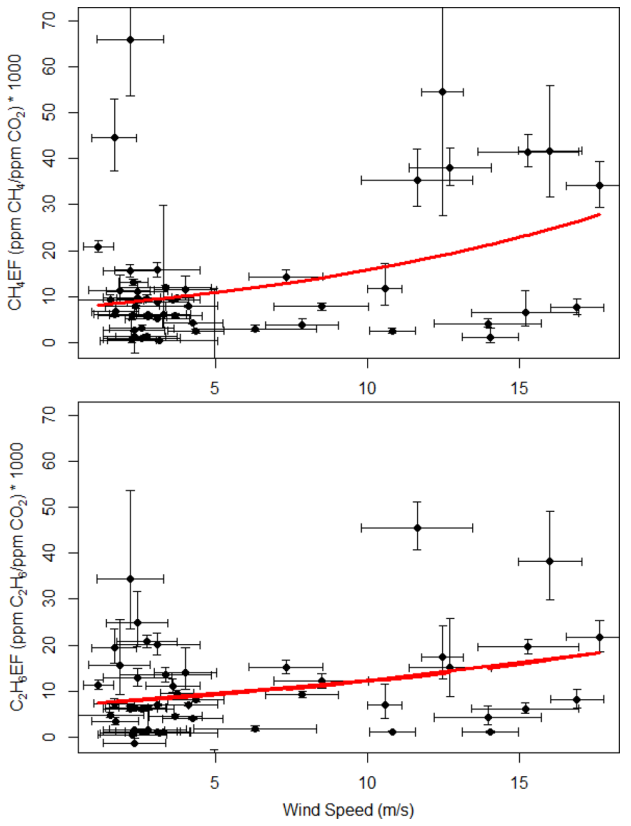

Figure 3. CH_4 and C_2H_6 EF plotted against wind speed for all plumes, with an exponential fit in red. Error bars represent 95% confidence intervals in EF and 1σ in wind speed.

Some flares were circled repeatedly or revisited on different days, and so we transected multiple plumes from the same flare. The calculated EF for the flare was not consistent between different plumes, suggesting fluctuation in the efficiency. Caulton et al. (2014) found large overall variability in CH_4 EF and inconsistency between sampling on different days but attribute the variability to the small sample size of their plumes.[20] Weyant et al. (2016) reported inconsistent emissions of BC for flares sampled on different days, and observed large variability in BC EF for multiple passes of the same flare, citing variability in gas flow rate and gas composition as possible sources.[21] From our data alone, we cannot resolve the cause of same-flare variability, but it is apparently a feature consistent across studies.

We did not observe a clear relationship between EF and wind speed for plumes from the same flare, possibly due to factors such as flow rate or exit velocity. For some flares that were sampled multiple times, we did not get a sharp, identifiable peak in CO_2 or CH_4 on every pass, and so we were not able to analyze all possible passes. The EF calculation included background points in the regression, removing these points from the fit and forcing the line through zero did not significantly affect the results. Comparing CH_4 and C_2H_6 emission factors for each plume, we found a linear relationship with a R^2 value of 0.57, as plumes with higher emissions of CH_4 had corresponding higher emissions of C_2H_6, suggesting that combustion efficiency is somewhat uniform across hydrocarbons.

Like Weyant et al. (2016),[21] we did not observe a dependence between BC emission factor and CH_4 EF for each plume. Elevated CH_4 emissions from a flare do not necessarily indicate higher or lower BC emission. Adding in an ethane term to eq 1 did not significantly change the BC EF

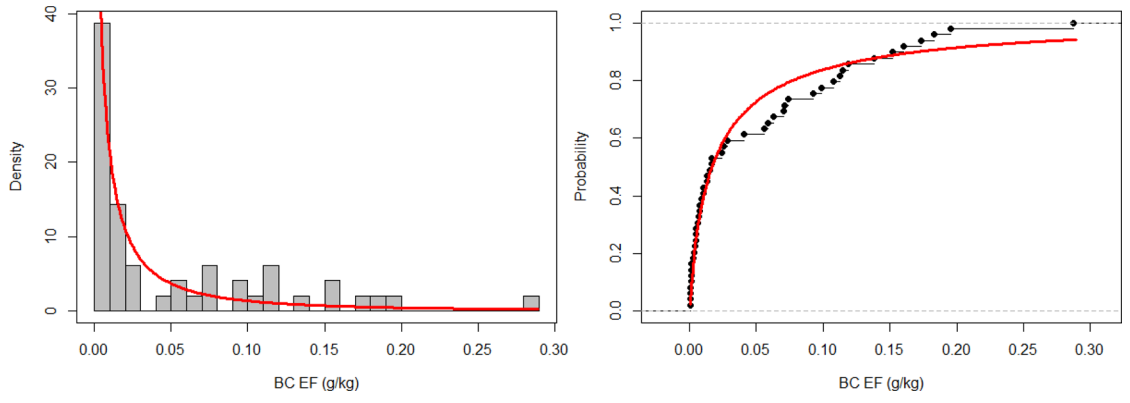

Figure 4. On the left, a histogram of black carbon emission factor for all flare plumes, with log-normal density (red line). On the right, distribution function of BC EF in black with log-normal distribution function in red.

DOI: 10.1021/acs.est.6b05183
Environ. Sci. Technol. 2017, 51, 5317−5325

calculation, as the ppm-order enhancement of CO_2 dominates the ppb-order enhancement of C_2H_6 and CH_4.

Figure 4 shows the distribution and probability function of BC emission factor in g BC/kg gas. The distribution is right-skewed, matching the results of Weyant et al. (2016),[21] and was fit with a log-normal density using a maximum-likelihood method. The log-normal distribution function is given by

$$f(x) = \frac{1}{\sqrt{(2\pi)}\sigma x} e^{-((\log x-\mu)^2/(2\sigma^2))} \quad (3)$$

μ and σ are the mean and standard deviation of the logarithm. A Pearson correlation analysis between the BC emission factor probability distribution and the log-normal distribution resulted in a correlation coefficient of 0.96. We present the log-normal fit as a way to illustrate the skewed distribution and provide a quantitative representation. Results derived from the combustion efficiency distribution use the raw distribution rather than an approximation with the log-normal fit.

We report BC EF from flares in g/kg, which is grams of BC produced per kilogram of hydrocarbons in the fuel gas. The values ranged from 0.0004 to 0.287 g/kg. We can convert from g/kg to g/m^3 using a flared gas density of 1.23 ± 0.14 kg/m^3,[40] allowing us to express BC EF in terms of gas flared volume and to compare the results with previous studies. Even with the observation of a right-skewed distribution, our analysis finds lower BC emissions than previously reported. Schwarz et al. (2015)[10] provided an estimate for all the BC sources in the Bakken of 0.57 ± 0.14 g/m^3. This upper bound on flaring is twice the highest emission value we observed (Figure 4). Similarly, laboratory analysis by McEwen et al. (2012)[22] reported emissions much larger than we observe (0.51 g/m^3, off scale in Figure 4). The mean value of 0.13 ± 0.36 g/m^3 measured with an SP2 by Weyant et al. (2016)[21] is within our observed range, though it falls within the top 20% of emitters we observed. Our observed in-field flares thus appear to have produced less BC than would be predicted from previous studies. The median, mean, and standard deviation of the mean BC emission factor we observed were 0.021 g/m^3 and 0.066 ± 0.009 g/m^3 (or 0.017 g/kg and 0.053 ± 0.008 g/kg), respectively, though given the skewed distribution care needs to be taken in interpreting these values. Given that 3.7 BCM of gas was flared in the Bakken field in 2014,[3] applying that to the entire distribution of BC EF in g/m^3 suggests total BC emissions from flaring of 0.24 Gg BC/year. However, the top quartile of flares contribute disproportionately, 0.17 Gg BC/year, which is 70% of the total emissions from flares. Overall, our emission rate of 0.24 Gg BC/year is two-thirds the rate of 0.36 Gg BC/year calculated by Weyant et al. (2016)[21] for flares and 17% of the total Bakken emission rate (1.4 Gg BC/year) reported by Schwarz et al. (2015).[10] Based on these results, using a single emission factor to estimate emissions from flares in a region does not properly represent the wide variability in emissions that may be present. Total emissions from flaring could potentially be substantially reduced if the least efficient flares alone are identified and addressed.

Combustion Efficiency. For methane and ethane, the percent of gas remaining provides a useful metric for flare efficiency; this is simply 100-DRE. In Figure 5 the distribution of percent remaining CH_4 and C_2H_6 is illustrated, and a log-normal relationship is apparent. As with emission factors, we found a linear relationship between CH_4 and C_2H_6 DRE for each plume, with a R^2 of 0.53.

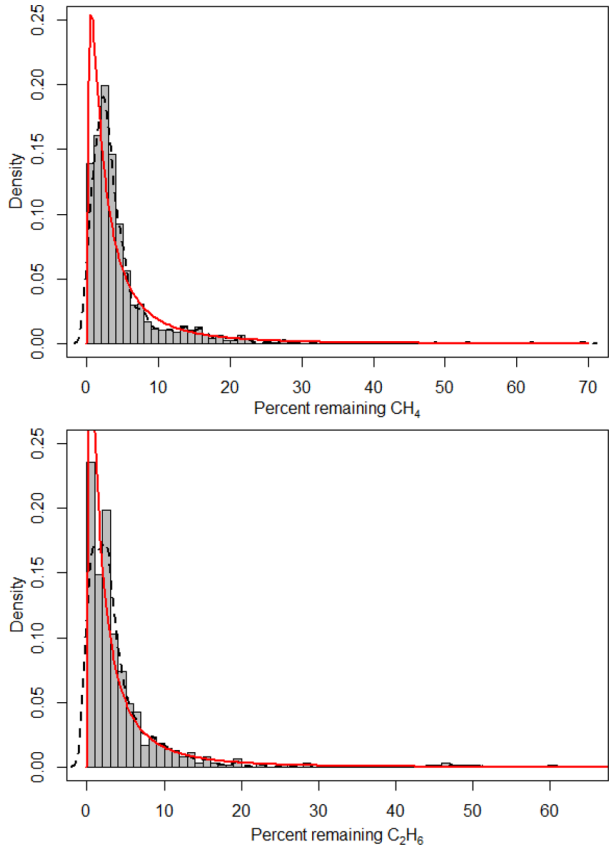

Figure 5. Histogram of remaining CH_4 and C_2H_6 (100-DRE) with density curve (dashed black) and log-normal fit (red). These distributions were integrated to calculate the emissions due to incomplete combustion.

A Pearson correlation analysis of the DRE probability distributions and the log-normal fit distribution produced a correlation coefficient of 0.99 for both CH_4 and C_2H_6. The distribution of CH_4 and C_2H_6 emission factors, which are theoretically consistent with the DRE calculations, also exhibit a skewed distribution though a log-normal relationship is not as apparent. The median DRE for CH_4 is 97.14 ± 0.37 using the integral method and 96.99 ± 0.23 using the aggregate data set. For C_2H_6 the median DRE is 97.33 ± 0.27 and 97.36 ± 0.25, respectively. These median values are close to the expected efficiency (98%), but the right-skewed distribution indicates that 98% is not a representative destruction efficiency and would overpredict methane and ethane destruction.

We can assess the impact of this observed skewed distribution by considering the contribution of incomplete flare combustion to total field methane and ethane emissions. Using aircraft data and a mass balance technique, Peischl et al. (2016)[31] calculated a methane flux for the Bakken region that extrapolates to an annual flux of 0.25 ± 0.05 Tg CH_4/year. As with black carbon, we can use reported flaring gas volumes for North Dakota in 2014[3] and integrate the distribution of observed DRE values to produce an estimated emission of methane from incomplete combustion of 0.052 Tg CH_4/year, or 21% ± 4% of the total emissions reported by Peischl et al. (2016), using the uncertainty bound on the flux calculation. This is more than double the contribution one would find if the expected value of 98% was assumed representative of the field, which would predict emissions representing 8% ± 1.6% of the total field emissions. Caulton et al. (2014) reported much-

DOI: 10.1021/acs.est.6b05183
Environ. Sci. Technol. 2017, 51, 5317−5325

higher combustion efficiencies, and applying their median 99.98% value would suggest only a fraction of a percent (0.13% ± 0.03%) of the total field emissions was from incomplete combustion in flares.

We performed the same analysis for ethane, and compareed with the total field emissions estimate of 0.23 ± 0.07 Tg C_2H_6/year reported in Kort et al. (2016).[32] Again our observed combustion efficiencies suggest incomplete combustion from flares contributes substantially to total field emissions, 17% ± 5% of the total emissions (0.039 Tg/year), more than double that predicted by using 98% as a representative value.

The observed log-normal distribution results in a disproportionate impact from flares exhibiting poor combustion efficiencies. We find the top quartile of methane emitters contribute 0.036 Tg CH_4/year, which is 69% of total emissions from incomplete flare combustion (and 14% of the total field emissions). Similarly, for ethane, the top quartile of emitters contributes 0.026 Tg C_2H_6/year, which is 66% of the total emissions from incomplete flare combustion (and 12% of total field emissions).

Why do we find higher methane emissions and lower black carbon emissions than other studies conducted in the Bakken shale?[10,20,21] We cannot definitively pinpoint the reason. We sampled in the same subregion of the Bakken as Caulton et al. (2014),[20] though we did not sample any of the same flares they did, and our campaign was 2 years after theirs. Weyant et al. (2016)[21] did not report specific flare locations but were likely in the same subregion as well 2 months before our campaign.

There is a difference in sampling methods that could contribute. Caulton et al. (2014) flew low and close to the flares, although specific altitudes and distances are not reported.[20] As we did not specifically target larger (and so potentially more-efficient) flares, our approach makes it more likely to sample higher-emitting flares. Weyant et al. (2016) also likely flew closer to the flares than we did, although at a slower speed (45 m/s) than at which we typically sampled (65 m/s).[21] We did not observe a clear correlation between sampling distance and combustion efficiency in our data, but it certainly affects variables such as plume entrainment, other emissions sources, turbulence, and environmental factors.

The largest source of discrepancy in results is likely that relatively few flares have been sampled: 26 (85 passes) by Weyant et al. (2016),[21] 10 by Caulton et al. (2014),[20] and 37 (52 passes) in our study, and thus, there is large representation error. In our study, we attempt a statistical sampling for greater representativeness, but given that there were over 5500 wells with reported flaring in the Bakken in 2014,[3] 37 independent flares only represents 0.6% of active flares. Thus, we think our results should be considered in concert with the Weyant and Caulton analyses, and our data should be considered in aggregate. In doing so, it would subtly change our total estimated contribution (lower for methane and higher for black carbon), but the observed log-normal distribution result would not change.

GLOBAL IMPLICATIONS

Our sampling provides sufficient statistics to observe a heavy-tail distribution of combustion efficiencies. This heavy-tail characteristic has been observed and reported for methane emissions from the oil and gas sector,[25−27,29,42] but this represents a first observation of the heavy-tail for flaring emissions of methane and ethane. This has important implications for current and future contributions from flaring activities. To illustrate, let us consider if our observed distribution were globally representative. Globally, 143 ± 13.6 BCM of gas is flared annually.[43] If 98% destruction removal efficiency were representative of every flare, that would correspond to a range in methane emissions of 1.14−1.90 Tg CH_4/year for a gas composition range of 60%−100% CH_4. Applying our observed distribution, that range changes to 2.78−4.64 Tg CH_4/year, more than doubling the amount emitted. In assessing the climate and air quality impacts of flaring, it is critical that skewed distributions are accounted for in the cases of methane, ethane, and black carbon. Although our specific observed emissions factors and efficiencies are likely only representative of the Bakken field, the observations of a skewed distribution is likely general.

AUTHOR INFORMATION

Corresponding Author

*Phone: (734) 764-7099; e-mail: agvak@umich.edu.

ORCID

Alexander Gvakharia: 0000-0003-1260-4744

Adam Brandt: 0000-0002-2528-1473

Notes

The authors declare no competing financial interest.

ACKNOWLEDGMENTS

Data from the aircraft campaign reported in the manuscript are archived and available at http://www.esrl.noaa.gov/csd/groups/csd7/measurements/2014topdown/. This project was supported by the NOAA AC4 program under grant no. NA14OAR0110139 and NASA grant no. NNX14AI87G. J.P. and T.R. were supported in part by the NOAA Climate Program Office and in part by the NOAA Atmospheric Chemistry, Carbon Cycle, and Climate Program. We thank NOAA Aircraft Operations Center staff and flight crew for their efforts in helping collect these data.

REFERENCES

(1) Elvidge, C. D.; Ziskin, D.; Baugh, K. E.; Tuttle, B. T.; Ghosh, T.; Pack, D. W.; Erwin, E. H.; Zhizhin, M. A Fifteen Year Record of Global Natural Gas Flaring Derived from Satellite Data. *Energies* **2009**, *2*, 595.

(2) U.S. Energy Information Administration. Natural Gas Gross Withdrawals and Production. https://www.eia.gov/dnav/ng/ng_prod_sum_a_EPG0_VGV_mmcf_a.htm (accessed on 4/13/2016).

(3) North Dakota State Government. North Dakota Drilling and Production Statistics. https://www.dmr.nd.gov/oilgas/stats/statisticsvw.asp (accessed on 4/13/2016).

(4) IPCC. In *Climate Change 2013: The Physical Science Basis. Contribution of Working Group I to the Fifth Assessment Report of the Intergovernmental Panel on Climate Change*; Stocker, T., Qin, D., Plattner, G.-K., Tignor, M., Allen, S., Boschung, J., Nauels, A., Xia, Y., Bex, V., Midgley, P., Eds.; Cambridge University Press: Cambridge, United Kingdom, 2013; Chapter SPM, p 1−30.

(5) Shindell, D. T.; Faluvegi, G.; Koch, D. M.; Schmidt, G. A.; Unger, N.; Bauer, S. E. Improved Attribution of Climate Forcing to Emissions. *Science* **2009**, *326*, 716−718.

(6) Ismail, O.; Umukoro, G. Global Impact of Gas Flaring. *Energy Power Eng.* **2012**, *4*, 290−302.

(7) Simpson, I. J.; Andersen, M. P. S.; Meinardi, S.; Bruhwiler, L.; Blake, N. J.; Helmig, D.; Rowland, F. S.; Blake, D. R. Long-term decline of global atmospheric ethane concentrations and implications for methane. *Nature* **2012**, *488*, 490−494.

(8) Bond, T. C.; Doherty, S. J.; Fahey, D. W.; Forster, P. M.; Berntsen, T.; DeAngelo, B. J.; Flanner, M. G.; Ghan, S.; Kärcher, B.;

DOI: 10.1021/acs.est.6b05183
Environ. Sci. Technol. 2017, 51, 5317−5325

Koch, D.; Kinne, S.; Kondo, Y.; Quinn, P. K.; Sarofim, M. C.; Schultz, M. G.; Schulz, M.; Venkataraman, C.; Zhang, H.; Zhang, S.; Bellouin, N.; Guttikunda, S. K.; Hopke, P. K.; Jacobson, M. Z.; Kaiser, J. W.; Klimont, Z.; Lohmann, U.; Schwarz, J. P.; Shindell, D.; Storelvmo, T.; Warren, S. G.; Zender, C. S. Bounding the role of black carbon in the climate system: A scientific assessment. *J. Geophys. Res., [Atmos]* **2013**, *118*, 5380−5552.

(9) Stohl, A.; Klimont, Z.; Eckhardt, S.; Kupiainen, K.; Shevchenko, V. P.; Kopeikin, V. M.; Novigatsky, A. N. Black carbon in the Arctic: the underestimated role of gas flaring and residential combustion emissions. *Atmos. Chem. Phys.* **2013**, *13*, 8833.

(10) Schwarz, J. P.; Holloway, J. S.; Katich, J. M.; McKeen, S.; Kort, E. A.; Smith, M. L.; Ryerson, T. B.; Sweeney, C.; Peischl, J. Black Carbon Emissions from the Bakken Oil and Gas Development Region. *Environ. Sci. Technol. Lett.* **2015**, *2*, 281−285.

(11) Anenberg, S. C.; Schwartz, J.; Shindell, D.; Amann, M.; Faluvegi, G.; Klimont, Z.; Janssens-Maenhout, G.; Pozzoli, L.; van Dingenen, R.; Vignati, E.; Emberson, L.; Muller, N. Z.; West, J. J.; Williams, M.; Demkine, V.; Hicks, W. K.; Kuylenstierna, J.; Raes, F.; Ramanathan, V. Global air quality and health co-benefits of mitigating near-term climate change through methane and black carbon emission controls. *Environ. Health Perspect.* **2012**, *120*, 831−839.

(12) The World Bank. Zero Routine Flaring by 2030. http://www.worldbank.org/en/programs/zero-routine-flaring-by-2030 (accessed on 4/13/2016).

(13) U.S. EPA Office of Air Quality Planning and Standards (OAQPS). Parameters for Properly Designed and Operated Flares. https://www3.epa.gov/airtoxics/flare/2012flaretechreport.pdf (accessed on 4/13/2016).

(14) Emission Standards Division. U.S. Environmental Protection Agency, Office of Air Radiation, OAQPS, Basis and Purpose Document on Specifications For Hydrogen-Fueled Flares. http://www.tceq.state.tx.us/assets/public/implementation/air/rules/Flare/Resource_5.pdf (accessed on 4/13/2016).

(15) Johnson, M.; Kostiuk, L. Efficiencies of low-momentum jet diffusion flames in crosswinds. *Combust. Flame* **2000**, *123*, 189−200.

(16) Johnson, M.; Kostiuk, L. A parametric model for the efficiency of a flare in crosswind. *Proc. Combust. Inst.* **2002**, *29*, 1943−1950.

(17) Leahey, D. M.; Preston, K.; Strosher, M. Theoretical and observational assessments of flare efficiencies. (Technical Paper). *J. Air Waste Manage. Assoc.* **2001**, *51*, 1610.

(18) Haus, R.; Wilkinson, R.; Heland, J.; Schafer, K. Remote sensing of gas emissions on natural gas flares. *Pure Appl. Opt.* **1998**, *7*, 853.

(19) Knighton, W. B.; Herndon, S. C.; Franklin, J. F.; Wood, E. C.; Wormhoudt, J.; Brooks, W.; Fortner, E. C.; Allen, D. T. Direct measurement of volatile organic compound emissions from industrial flares using real-time online techniques: Proton Transfer Reaction Mass Spectrometry and Tunable Infrared Laser Differential Absorption Spectroscopy. *Ind. Eng. Chem. Res.* **2012**, *51*, 12674−12684.

(20) Caulton, D. R.; Shepson, P. B.; Cambaliza, M. O.; McCabe, D.; Baum, E.; Stirm, B. H. Methane Destruction Efficiency of Natural Gas Flares Associated with Shale Formation Wells. *Environ. Sci. Technol.* **2014**, *48*, 9548−9554.

(21) Weyant, C. L.; Shepson, P. B.; Subramanian, R.; Cambaliza, M. O. L.; Heimburger, A.; McCabe, D.; Baum, E.; Stirm, B. H.; Bond, T. C. Black Carbon Emissions from Associated Natural Gas Flaring. *Environ. Sci. Technol.* **2016**, *50*, 2075−2081.

(22) McEwen, J. D. N.; Johnson, M. R. Black carbon particulate matter emission factors for buoyancy-driven associated gas flares. *J. Air Waste Manage. Assoc.* **2012**, *62*, 307−321.

(23) Kahforoushan, D.; Fatehifar, E.; Soltan, J. The Estimation of CO2 Emission Factors for Combustion Sources in Oil and Gas Processing Plants. *Energy Sources, Part A* **2010**, *33*, 202−210.

(24) Brandt, A. R.; Heath, G. A.; Kort, E. A.; O'Sullivan, F.; Pétron, G.; Jordaan, S. M.; Tans, P.; Wilcox, J.; Gopstein, A. M.; Arent, D.; Wofsy, S.; Brown, N. J.; Bradley, R.; Stucky, G. D.; Eardley, D.; Harriss, R. Methane Leaks from North American Natural Gas Systems. *Science* **2014**, *343*, 733−735.

(25) Yuan, B.; Kaser, L.; Karl, T.; Graus, M.; Peischl, J.; Campos, T. L.; Shertz, S.; Apel, E. C.; Hornbrook, R. S.; Hills, A.; Gilman, J. B.; Lerner, B. M.; Warneke, C.; Flocke, F. M.; Ryerson, T. B.; Guenther, A. B.; de Gouw, J. A. Airborne flux measurements of methane and volatile organic compounds over the Haynesville and Marcellus shale gas production regions. *J. Geophys. Res., [Atmos.]* **2015**, *120*, 6271−6289.

(26) Mitchell, A. L.; Tkacik, D. S.; Roscioli, J. R.; Herndon, S. C.; Yacovitch, T. I.; Martinez, D. M.; Vaughn, T. L.; Williams, L. L.; Sullivan, M. R.; Floerchinger, C.; Omara, M.; Subramanian, R.; Zimmerle, D.; Marchese, A. J.; Robinson, A. L. Measurements of Methane Emissions from Natural Gas Gathering Facilities and Processing Plants: Measurement Results. *Environ. Sci. Technol.* **2015**, *49*, 3219−3227.

(27) Allen, D. T. Methane emissions from natural gas production and use: reconciling bottom-up and top-down measurements. *Curr. Opin. Chem. Eng.* **2014**, *5*, 78−83.

(28) Brandt, A. R.; Heath, G. A.; Cooley, D. Methane Leaks from Natural Gas Systems Follow Extreme Distributions. *Environ. Sci. Technol.* **2016**, *50*, 12512−12520.

(29) Frankenberg, C.; Thorpe, A. K.; Thompson, D. R.; Hulley, G.; Kort, E. A.; Vance, N.; Borchardt, J.; Krings, T.; Gerilowski, K.; Sweeney, C.; Conley, S.; Bue, B. D.; Aubrey, A. D.; Hook, S.; Green, R. O. Airborne methane remote measurements reveal heavy-tail flux distribution in Four Corners region. *Proc. Natl. Acad. Sci. U. S. A.* **2016**, *113*, 9734−9739.

(30) Allen, D. T.; Smith, D.; Torres, V. M.; Saldaña, F. C. Carbon dioxide, methane and black carbon emissions from upstream oil and gas flaring in the United States. *Curr. Opin. Chem. Eng.* **2016**, *13*, 119−123. SI:13 Energy and Environmental Engineering/Reaction engineering and catalysis 2016.

(31) Peischl, J.; Karion, A.; Sweeney, C.; Kort, E. A.; Smith, M. L.; Brandt, A. R.; Yeskoo, T.; Aikin, K. C.; Conley, S. A.; Gvakharia, A.; Trainer, M.; Wolter, S.; Ryerson, T. B. Quantifying atmospheric methane emissions from oil and natural gas production in the Bakken shale region of North Dakota. *J. Geophys. Res., [Atmos.]* **2016**, *121*, 6101−6111.

(32) Kort, E. A.; Smith, M. L.; Murray, L. T.; Gvakharia, A.; Brandt, A. R.; Peischl, J.; Ryerson, T. B.; Sweeney, C.; Travis, K. Fugitive emissions from the Bakken shale illustrate role of shale production in global ethane shift. *Geophys. Res. Lett.* **2016**, *43*, 4617−4623.

(33) Karion, A.; Sweeney, C.; Kort, E. A.; Shepson, P. B.; Brewer, A.; Cambaliza, M.; Conley, S. A.; Davis, K.; Deng, A.; Hardesty, M.; Herndon, S. C.; Lauvaux, T.; Lavoie, T.; Lyon, D.; Newberger, T.; Pétron, G.; Rella, C.; Smith, M.; Wolter, S.; Yacovitch, T. I.; Tans, P. Aircraft-Based Estimate of Total Methane Emissions from the Barnett Shale Region. *Environ. Sci. Technol.* **2015**, *49*, 8124−8131.

(34) Karion, A.; Sweeney, C.; Wolter, S.; Newberger, T.; Chen, H.; Andrews, A.; Kofler, J.; Neff, D.; Tans, P. Long-term greenhouse gas measurements from aircraft. *Atmos. Meas. Tech.* **2013**, *6*, 511.

(35) Yacovitch, T. I.; Herndon, S. C.; Roscioli, J. R.; Floerchinger, C.; McGovern, R. M.; Agnese, M.; Pétron, G.; Kofler, J.; Sweeney, C.; Karion, A.; Conley, S. A.; Kort, E. A.; Nähle, L.; Fischer, M.; Hildebrandt, L.; Koeth, J.; McManus, J. B.; Nelson, D. D.; Zahniser, M. S.; Kolb, C. E. Demonstration of an Ethane Spectrometer for Methane Source Identification. *Environ. Sci. Technol.* **2014**, *48*, 8028−8034.

(36) Smith, M. L.; Kort, E. A.; Karion, A.; Sweeney, C.; Herndon, S. C.; Yacovitch, T. I. Airborne ethane observations in the Barnett Shale: Quantification of ethane flux and attribution of methane emissions. *Environ. Sci. Technol.* **2015**, *49*, 8158−8166.

(37) Schwarz, J. P.; Spackman, J. R.; Gao, R. S.; Perring, A. E.; Cross, E.; Onasch, T. B.; Ahern, A.; Wrobel, W.; Davidovits, P.; Olfert, J.; Dubey, M. K.; Mazzoleni, C.; Fahey, D. W. The Detection Efficiency of the Single Particle Soot Photometer. *Aerosol Sci. Technol.* **2010**, *44*, 612−628.

(38) Conley, S. A.; Faloona, I. C.; Lenschow, D. H.; Karion, A.; Sweeney, C. A Low-Cost System for Measuring Horizontal Winds

DOI: 10.1021/acs.est.6b05183
Environ. Sci. Technol. 2017, 51, 5317−5325

from Single-Engine Aircraft. *J. Atmos. Oceanic Technol.* **2014**, *31*, 1312−1320.
(39) Zannetti, P. *Air Pollution Modeling*, 1st ed.; Springer US: New York City, New York, 1990.
(40) Brandt, A. R.; Yeskoo, T.; McNally, M. S.; Vafi, K.; Yeh, S.; Cai, H.; Wang, M. Q. Energy Intensity and Greenhouse Gas Emissions from Tight Oil Production in the Bakken Formation. *Energy Fuels* **2016**, *30*, 9613−9621.
(41) Beychok, M. R. *Fundamentals Of Stack Gas Dispersion*, 4th ed.; Milton R. Beychok: Irvine, CA, 2005; pp 1−193.
(42) Subramanian, R.; Williams, L. L.; Vaughn, T. L.; Zimmerle, D.; Roscioli, J. R.; Herndon, S. C.; Yacovitch, T. I.; Floerchinger, C.; Tkacik, D. S.; Mitchell, A. L.; Sullivan, M. R.; Dallmann, T. R.; Robinson, A. L. Methane Emissions from Natural Gas Compressor Stations in the Transmission and Storage Sector: Measurements and Comparisons with the EPA Greenhouse Gas Reporting Program Protocol. *Environ. Sci. Technol.* **2015**, *49*, 3252−3261.
(43) Elvidge, C. D.; Zhizhin, M.; Baugh, K.; Hsu, F.-C.; Ghosh, T. Methods for Global Survey of Natural Gas Flaring from Visible Infrared Imaging Radiometer Suite Data. *Energies* **2016**, *9*, 14.

DOI: 10.1021/acs.est.6b05183
Environ. Sci. Technol. 2017, 51, 5317−5325